Somatostatin Receptor-Binding Peptides Suitable for Tumor Radiotherapy with Re-188 or Re-186. Chemistry and Initial Biological Studies

John E. Cyr,*[,∇,§] Daniel A. Pearson,[∇,⊥] David M. Wilson,[∇,#] Carol A. Nelson,[∇,⊗] Mary Guaraldi,[∇,+] Michael T. Azure,[∇,+] John Lister-James,[∇,‡] Ludger M. Dinkelborg,[†,Δ] and Richard T. Dean[∇,‡]

Diatide Research Laboaratories, 9 Delta Dr., Londonderry, New Hampshire 03053 and Research Laboratories of Schering AG, 178 Muellerstrasse, Berlin 13342, Germany

Received November 3, 2006

Somatostatin derivative peptides previously designed for radiodiagnostic purposes (^{99m}Tc P829 or ^{99m}Tc depreotide) were reoptimized for radiotherapy of tumors with rhenium radioisotopes. An optimized pharmacophore peptide P1839 was derived by *in vitro* binding affinity assay to AR42J rat pancreatic tumor cell membranes. Peptides with chelating domains and their oxorhenium(V) complexes were tested *in vitro* for binding to NCI H69 human SCLC tumor membranes. Further optimization entailed radiolabeling with ^{99m}Tc and biodistribution in an AR42J xenograft mouse model. Kidney uptake was decreased substantially by removing positively charged residues. Neutral N_3S diamide amine thiol chelators with no adjacent positive charges had the best overall properties. Substituting an aromatic amino acid into the chelator approximately doubled the tumor uptake. The final optimized peptide P2045 (**39**) radiolabeled with ^{99m}Tc exhibited increased tumor uptake (∼25 %ID/g at 1.5 h), lower kidney uptake (∼4.8 %ID/g at 1.5 h), and extensive urinary excretion (59 %ID at 1.5 h). Finally, comparison biodistribution studies between ^{99m}Tc and ^{188}Re (**39**) showed a good correlation between the two metal complexes and demonstrated prolonged tumor retention (≥24 h).

Introduction

Somatostatin (somatotropin release-inhibiting factor, SRIF-14)[a] is a tetradecapeptide secreted by neuroendocrine, inflammatory, and immune cells in response to various stimuli.[1] The potent effects of somatostatin on various secretory processes are mediated through its specific high-affinity binding to somatostatin receptors (SSTRs), of which there are five subtypes.[2] SSTRs have been found to be overexpressed in a wide range of tumor types including those of the brain, digestive tract, pancreas, lung, thyroid, mammary gland, prostate, lymph system, and ovary.[3] SSTR overexpression has also been demonstrated on the peritumoral veins of a number of human tumors.[4]

SRIF-14 (**1**; Figure 1) was shown to have an inhibitory effect on the growth of various tumors, but its efficacy was hampered by its short biological half-life of about 3 min. Stabilized analogues were developed, leading to the commercial therapeutic peptide octreotide (**2**, SMS 201-995), which more recently has become available in a slow release formulation.[5]

The overexpression of SSTR by some tumors also provides the basis for imaging cancerous from other tissues by the administration of SSTR-binding radiotracers followed by gamma-camera scintigraphy. On the basis of this principle, pentetreotide (**3**) labeled with In-111 ([^{111}In-DTPA^0]octreotide) is approved for the detection of SSTR-expressing neuroendocrine tumors,[6] and depreotide labeled with Tc-99m (**4**) is approved for the detection of SSTR-expressing pulmonary masses.[7] The structures of these two peptides are shown in Figure 2.

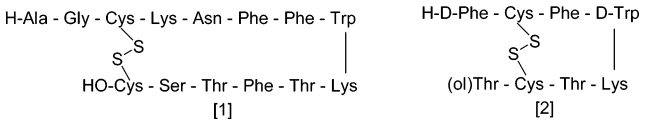

Figure 1. Native somatostatin (**1**) and a stabilized analogue peptide for therapy: octreotide (**2**).

As a natural extension to the diagnostic applications of somatostatin analogues radiolabeled with gamma-emitting radioisotopes, SSTR-binding compounds labeled with radioisotopes having therapeutically useful emissions are being considered for the treatment of SSTR-expressing tumors. Most radiotherapeutic agents reported to date are octreotide/octreotate analogues targeting predominantly SSTR2,[8,9,10−13] although more recently, promising new analogues with affinity for the other four SSTR subtypes as well have been reported.[14] Y-90-DOTA-Tyr^3-octreotide (DOTATOC)[15] and Lu-177-Tyr^3-octreotate (LuTate)[16] have been evaluated in humans to treat neuroendocrine tumors and have demonstrated promising therapeutic efficacy.

We have previously developed the Tc-99m somatostatin analogue Tc-99m depreotide for diagnosis of malignant lung cancer[17] and were interested in expanding this work to use the same class of peptides for radiotherapy. Although there are no isotopes of technetium suitable for radiotherapy, it was expected that the already-established Tc metal chelation chemistry of the depreotide-type peptides could be adopted for rhenium isotopes, owing to the similar chemistries of technetium and rhenium.[18] Furthermore, both Re-188 and Re-186 have β-emissions suitable for killing tumor cells. Re-188 is preferred because it has

* Corresponding author. E-mail: john_cyr@berlex.com.
∇ Diatide Research Laboaratories.
† Schering AG.
§ Current address: Berlex Biosciences, 2600 Hilltop Dr., Richmond, CA 94804.
⊥ Current address: Vertex Pharmaceuticals, 130 Waverly St., Cambridge, MA 02139.
Current address: Palatin Technologies, 4-C Cedar Brook Dr., Cranbury, NJ 08512.
⊗ Current address: Genzyme Corporation, 153 2nd Ave., Waltham, MA 02142.
+ Current address: Bristol Myers Squibb Medical Imaging, 331 Treble Cove Rd, N. Billerica, MA 01862.
‡ Current address: Xanthus Pharmaceuticals, 300 Technology Sq, Cambridge, MA 02139.
Δ Current address: Bayer Schering Pharma, Global Drug Discovery, 178 Muellerstrasse, Berlin 13342, Germany.

[a] Abbreviations: DMF, dimethylformamide; HATU, 1-hydroxy-7-azabenzotriazole; ID, injected dose; ReO, rhenium oxo; SCLC, small cell lung cancer; SRIF, somatotropin release-inhibiting factor; SSTR, somatostatin receptor; TFA, trifluoroacetic acid.

10.1021/jm061290i CCC: $37.00
Published on Web 02/22/2007

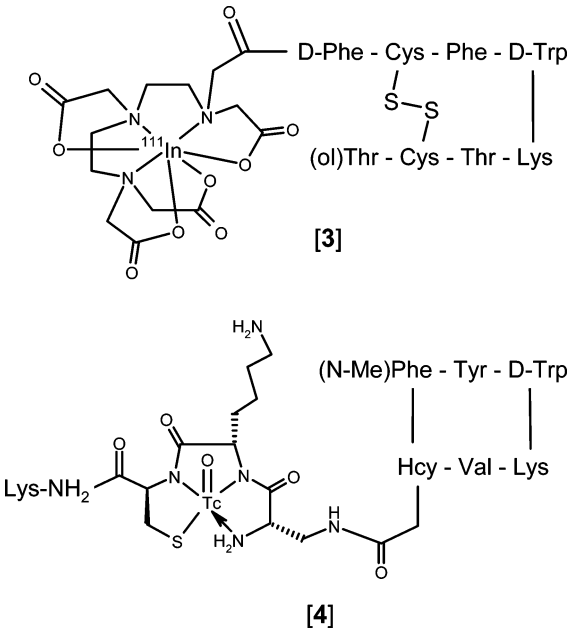

Figure 2. Radiolabeled somatostatin analogue peptides approved for diagnostic imaging of tumors. In-111 pentetreotide **(3)** for neuroendocrine tumors and Tc-99m depreotide (**4**) for lung tumors.

physical properties (half-life = 16.9 h; β^- emission maximum energy = 2 MeV; average energy = 764 keV) well-suited to radiotherapy and can be conveniently produced in high specific activity from a clinical generator.[19] Radiopharmaceutical compounds containing Re-188 have been evaluated clinically in a variety of therapeutic areas.[20] In addition, Re-188 has already been used to radiolabel peptides for targeted radiotherapy.[21,22,13] Re-186 has a longer half-life and a lower energy β^--emission than Re-188 and is produced at low specific activity in a nuclear reactor.

As a first look at the suitability of depreotide-type peptides for radiotherapy, Re-188 depreotide was evaluated in a tumor regression study in mice bearing AR42J rat pancreatic tumor xenografts. Although the radiolabeling was successful and tumor-growth was arrested, the tumor regression study showed unacceptably high radiotoxicity in nontarget organs (kidney, spleen, marrow).[23] Hence, it was clear that the depreotide peptide designed as a diagnostic was not optimized for radiotherapy and that modifications to the peptide were needed. The results of our studies to optimize the tumor uptake and biodistribution of high-affinity somatostatin receptor-binding peptides complexed to rhenium for cancer radiotherapy are presented in this paper.

The ideal radiotherapeutic agent should not only localize to sites of tumor with high selectivity but also have suitable pharmacokinetics to ensure rapid whole body clearance. A combination of optimal biodistribution and suitable pharmacokinetics reduces radiolytic damage to nontarget tissues and organs. In the field of radiotherapy, nontarget tissue damage for radiotherapeutic peptides has been a major issue, with the kidneys being the main nontarget organs of concern.[24] In an effort to minimize kidney uptake and increase the maximum tolerated dose, clinical researchers have resorted to infusions of cationic amino acids during radiotherapy to lower the uptake of radiopeptides in the kidneys.[25] The aforementioned radiotherapy studies with Re-188 depreotide showed unacceptable radiotoxicity largely due to the high uptake and retention of

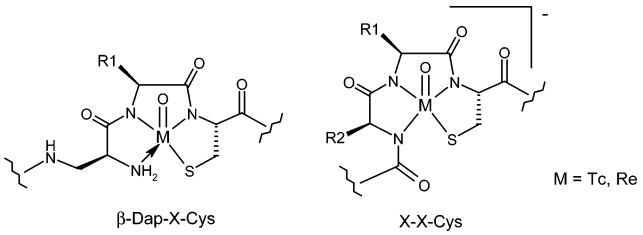

Figure 3. Peptide-based Tc/Re chelators evaluated in this work.

Table 1. Cyclic Peptide Pharmacophores

structure	compd no.	code
cyclo-[Hcy.(N-Me)F.YwKV]	**10**	P334
cyclo-[Hcy.(N-Me)F.YwKT]	**11**	P779
cyclo-[(N-Me)F.Hcy.YwKT]	**12**	P1835
cyclo-[F.(N-Me)Hcy.YwKT]	**13**	P1839
cyclo-[F.(N-Me)Hcy.YwKV]	**14**	P1840

the radiolabeled peptide (>100% ID/g) in the kidneys. Hence, lowering kidney uptake was one of the primary goals of this work.

The radiolabeled peptides described here complex the radiometal through peptide-based chelators comprised of a cysteine plus two other amino acids. Figure 3 depicts the structures of the metal chelate portions of the radiopeptides, in which the chelator consists of either the peptide sequence β-Dap-X-Cys or X-X-Cys (where X is any noncyclic α-amino acid). The Tc/Re metal is in the +5 oxidation state with an oxo oxygen ligand and "N_3S" coordination to the peptide-based chelator.[26] Three of the four donor atoms to the metal in the peptide chelator come from the alpha nitrogens of the amino acid residues (N_3), and the fourth donor atom comes from a cysteine side-chain sulfhydryl (S). Because the chelators used are peptidyl in nature, they can be conveniently altered by systematic changes in chelator amino acids X during peptide synthesis. In the work described here, mainly changes to the peptides in the chelator region were investigated and found to have profound effects on the bioefficacy of the radiopeptides.

Chemistry

The peptide agents described below in general were composed of a cyclic hexapeptide pharmacophore linked to a tetra- or pentapeptide containing an amino acid sequence amenable for complexation to Tc/Re. The pharmacophore and chelator moieties were prepared separately and subsequently conjugated via a reaction between a thiol located on the pharmacophore portion and a chloroacetyl group located on the chelator portion.

Pharmacophores. The cyclic receptor-binding pharmacophore moieties (Table 1) were synthesized by the solid-phase Fmoc method[27] as shown in Scheme 1. Chlorotrityl resin was used as the solid-phase support.[28] This acid-labile resin was chosen due to the very mild conditions required to cleave the protected peptide from the resin prior to cyclization. It was found that hexafluoroisopropanol was sufficiently acidic for this purpose. Because the peptide was easily and quickly cleaved from the chlorotrityl resin, an additional advantage was realized: the progress of the synthesis during intermediate stages could be monitored by analytical HPLC analysis. This was particularly important for the sterically demanding coupling between the resin-supported *N*-methylhomocysteine and Fmoc-phenylalanine, where monitoring the coupling efficiency by the ninhydrin method was rendered inoperative due to the presence of a secondary amine at the N-terminus. It was found that the use of HATU reagent[29] was required to affect this coupling. After cleavage of the protected peptide from the resin, HATU

Scheme 1. Synthesis of Pharmacophore Peptide **13**

H-Thr(tBu)-ClTrt resin
↓ 1. Fmoc-Lys(Boc)-OH, HBTU, DIEA 2. piperidine
H-Lys(Boc)-Thr(tBu)-ClTrt resin
↓ 1. Fmoc-D-Trp(Boc)-OH, HBTU, DIEA 2. piperidine
H-D-Trp(Boc)-Lys(Boc)-Thr(tBu)-ClTrt resin
↓ 1. Fmoc-Tyr(tBu)-OH, HBTU, DIEA 2. piperidine
H-Tyr(tBu)-D-Trp(Boc)-Lys(Boc)-Thr(tBu)-ClTrt resin
↓ 1. Fmoc-(N-Me)Hcy(Trt)-OH, HATU, DIEA 2. piperidine
H-(N-Me)Hcy(Trt)-Tyr(tBu)-D-Trp(Boc)-Lys(Boc)-Thr(tBu)-ClTrt resin
↓ 1. Fmoc-Phe-OH, HATU, DIEA 2. piperidine 3. 1:4 hexafluoro-2-propanol/DCM
H-Phe-(N-Me)Hcy(Trt)-Tyr(tBu)-D-Trp(Boc)-Lys(Boc)-Thr(tBu)-OH
↓ 1. HATU, DIEA 2. TFA/H_2O/TIPS/EDT 3. HPLC purification
cyclo-[Phe-(N-Me)Hcy-Tyr-D-Trp-Lys-Thr] [**13**]

Table 2. Chloroacetyl Chelator Precursors

structure	compd no.	code
$ClCH_2CO$.β-Dap(Boc).K(Boc).C(Trt).T(tBu)(ol)	**15**	
$ClCH_2CO$.GG.C(Trt).H.amide	**16**	
$ClCH_2CO$.TGG.C(Trt).amide	**17**	
$ClCH_2CO$.S.K.C(Trt).amide	**18**	
$ClCH_2CO$.β-Dap.K.C(Trt).amide	**19**	
$ClCH_2CO$.β-Dap(Boc).G.C(Trt).T(ol)	**20**	
$ClCH_2CO$.β-Dap(Boc).S(tBu).C(Trt).T(tBu)(ol)	**21**	
$ClCH_2CO$.β-Dap.Y.C(Trt).T(ol)	**22**	
$ClCH_2CO$.β-Dap(Boc).F(4-NHBoc).C(Trt).T(tBu)(ol)	**23**	
$ClCH_2CO$.β-Dap(Boc).F(4-NHBoc).C(Trt).T(tBu)	**24**	
$ClCH_2CO$.β-Dap.F(4-NH_2).C(Trt).TS	**25**	P2063

reagent was also found to be useful for the cyclization reaction. The crude cyclic peptides were treated with 95:5:2.5:2 TFA/water/triisopropylsilane/ethanedithiol followed by HPLC purification to obtain the deprotected cyclic peptides **10**−**14**. All peptides were >95% pure by HPLC peak analysis and had the expected MH+ peak when analyzed by mass spectrometry (Supporting Information, Table S1).

Chelators. Peptides containing the chelator moiety (Table 2) were also synthesized by solid-phase methodology as shown in Scheme 2 for compound **25**. For peptides in which the C-terminal functional group was either a carboxylic acid or an alcohol, chlorotrityl resin was used as the support. For peptides in which the C-terminal functional group was a carboxamide, Rink amide resin[30] was used. Peptides were cleaved from the resin using either hexafluoroisopropanol, as before, or 95:5 (v/v) TFA/water. In the cases where hexafluoroisopropanol was used, the recovered peptides were fully protected. In the cases where TFA was used the *tert*-butyl-based protecting groups were removed and, by adapting the workup conditions, the thiol group was selectively reprotected with a trityl group. This was accomplished by removing the TFA and water of the cleavage mixture *in vacuo* followed by dissolution of the crude peptide in chloroform, which was also removed *in vacuo*. After several such treatments with chloroform, all of the residual acid was removed with concomitant reattachment of the trityl group to the cysteine SH. All chloroacetyl peptides were >90% pure by

Scheme 2. Synthesis of Chloroacetyl Chelator Precursor **25**

H-Ser(tBu)-ClTrt resin
↓ 1. Fmoc-Thr(tBu)-OH, HBTU, DIEA 2. piperidine
H-Thr(tBu)-Ser(tBu)-ClTrt resin
↓ 1. Fmoc-Cys(Trt)-OH, DIC, HOBt 2. piperidine
H-Cys(Trt)-Thr(tBu)-Ser(tBu)-ClTrt resin
↓ 1. Fmoc-Phe(4-NHBoc)-OH, HBTU, DIEA 2. piperidine
H-Phe(4-NHBoc)-Cys(Trt)-Thr(tBu)-Ser(tBu)-ClTrt resin
↓ 1. Boc-Dap(Fmoc)-OH, HBTU, DIEA 2. piperidine
H-β-Dap(Boc)-Phe(4-NHBoc)-Cys(Trt)-Thr(tBu)-Ser(tBu)-ClTrt resin
↓ $ClCH_2CO_2H$, HBTU, DIEA
$ClCH_2CO$-β-Dap(Boc)-Phe(4-NHBoc)-Cys(Trt)-Thr(tBu)-Ser(tBu)-ClTrt resin
↓ 1. TFA/H_2O 2. Remove TFA and water with $CHCl_3$ 3. HPLC purification
$ClCH_2CO$-β-Dap-Phe(4-NH_2)-Cys(Trt)-Thr-Ser-OH [**25**]

Table 3. Pharmacophore−Chelator Conjugates

structure[a]	compd no.	code
11-CH_2CO.β-Dap.KCK.amide	**26**	
11-CH_2CO.β-Dap.KC.T(ol)	**27**	
13-CH_2CO.GGCH.amide	**28**	
13-CH_2CO.TGGC.amide	**29**	
13-CH_2CO.GGCR.amide	**30**	
13-CH_2CO.SKC.amide	**31**	
13-CH_2CO.β-Dap.KC.amide	**32**	
13-CH_2CO.β-Dap.GC.T(ol)	**33**	
13-CH_2CO.β-Dap.KC.T(ol)	**34**	
13-CH_2CO.β-Dap.SC.T(ol)	**35**	
13-CH_2CO.β-Dap.YC.T(ol)	**36**	
13-CH_2CO.β-Dap.F(4-NH_2).C.T(ol)	**37**	
13-CH_2CO.β-Dap.F(4-NH_2).CT	**38**	
13-CH_2CO.β-Dap.F(4-NH_2).CTS	**39**	P2045
10-CH_2CO.β-Dap.KCK.amide	**40**	P829
10-CH_2CO.GGCR.amide	**41**	

[a] Pharmacophore sequences are described in Table 1.

HPLC peak analysis and had the expected MH+ peak when analyzed by mass spectrometry (Supporting Information, Table S2).

Pharmacophore−Chelator Conjugates (Final Peptides). Pharmacophore−chelator conjugates (Table 3) were efficiently produced by mixing an equalmolar quantity of each in an acetonitrile/carbonate buffer solution at pH = 10.0, as shown in Scheme 3. The progress of the reaction was followed by analytical HPLC and the reaction quenched at the time of completion with aqueous TFA. The solution was concentrated and the trityl protecting group removed with TFA using triisopropylsilane as a trityl carbocation scavenger.[31] The final products were purified by HPLC to >95% purity and were confirmed by mass spectrometry (Supporting Information, Table S3).

Rhenium Oxo Complexes of the Final Peptides. Nonradioactive rhenium oxo complexes of the pharmacophore−chelator conjugate peptides were prepared by reacting the peptide with a 1.5 fold molar excess of $Bu_4NReOCl_4$ or $Bu_4NReOBr_4$ in anhydrous DMF at room temperature according

Scheme 3. Synthesis of Pharmacophore−Chelator Conjugate **39**

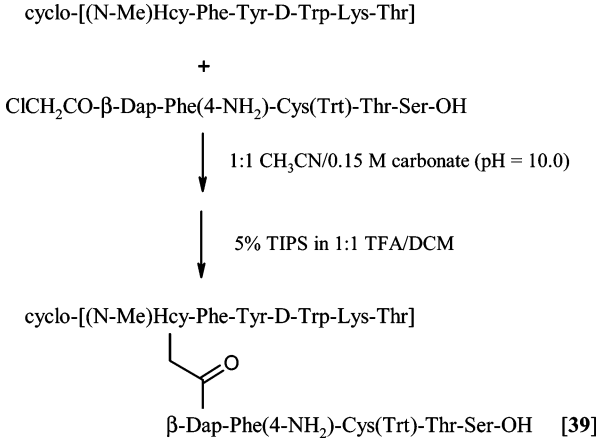

Table 4. *In Vitro* Binding of Pharmacophore Peptides to AR42J Rat Pancreatic Tumor Membranes

pharmacophore	compd no.	IC_{50} (nM)
cyclo-[YwKV.Hcy.(N-Me)F]	**10**	1.5
cyclo-[YwKT.Hcy.(N-Me)F]	**11**	0.4
cyclo-[YwKT.(N-Me)F.Hcy]	**12**	23.7
cyclo-[YwKTF.(N-Me)Hcy]	**13**	0.1
cyclo-[YwKVF.(N-Me)Hcy]	**14**	0.7

to published procedures.[17a] The [ReO] products were isolated by reversed phase preparative HPLC. All rhenium complexes were >95% pure by HPLC peak analysis.

Tc-99m and Re-188 Radiolabeling. The technetium-99m complexes of compounds **26**−**41** were prepared by reducing $^{99m}TcO_4^-$ with stannous tin at pH 6−7.4 in the presence of the peptide (ligand) and glucoheptonate (exchange ligand). The Re-188 complex of peptide **39** was prepared by a procedure similar to that of the Tc-99m radiolabelings, except that a larger amount of stannous tin was needed to reduce the rhenium. In addition, ascorbic acid and gentisate were added after the radiolabeling reaction was complete as radiolytic stabilizers. The radiochemical purity (RCP) of the radiolabeled complexes was measured by thin-layer chromatography (TLC) and analytical reversed phase HPLC. In all cases, the TLC RCP was greater than 90%, and the HPLC RCP was greater than 85%.

Biology

Several cyclic pharmacophore peptides were evaluated for their ability to target SSTR *in vitro*. Pharmacophores **10**−**14** were tested for SSTR-binding affinities using AR42J rat pancreatic tumor cell membranes, which are known to overexpress SSTR (predominantly the somatostatin receptor subtype 2, SSTR2[32]). The pharmacophore *in vitro* results are presented in Table 4. In order to ensure relevance in the treatment of human disease, several of the final drug candidate peptides (pharmacophore−chelator conjugates) and in addition rhenium oxo complexes of the peptides were tested for *in vitro* binding affinity to human SCLC NCI-H69 tumor membranes (which also overexpress SSTR2[33]). These results are given in Table 5. SSTR binding was assessed as the concentration of compound required to inhibit the specific binding of [^{125}I-Tyr-11]SRIF-14 to the tumor cell membranes by 50% (IC_{50}).[34] All compounds were tested in duplicate at five different concentrations.

The final drug candidate peptides (pharmacophore−chelator conjugates) were radiolabeled and evaluated for tumor uptake and biodistribution *in vivo*. The technetium-99m complexes of compounds **26**−**39** were administered to AR42J tumor xenograft-bearing athymic nude mice intravenously, and tumor,

Table 5. *In Vitro* Binding Affinities of SSTR Peptides and Rhenium Complexes to NCI-H69 Tumor Cell Membranes. Value in Parentheses Reflects Binding to a Secondary Site

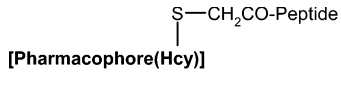

Pharmacophore
13 = cyclo-[F.(N-Me)Hcy.YwKV]
11 = cyclo-[Hcy.(N-Me)F.YwKT]
10 = cyclo-[Hcy.(N-Me)F.YwKV]

compound	compd no.	IC_{50} (nM) free peptide	IC_{50} (nM) ReO complex
13-CH_2CO.β-Dap.F(4-NH_2).C.TS	**39**	0.20 (8.91)	0.23 (14.7)
13-CH_2CO.β-Dap.F(4-NH_2).C.T	**38**	0.64 (6.41)	0.45
13-CH_2CO.β-Dap.F(4-NH_2).C.T(ol)	**37**	0.50	0.12 (430)
13-CH_2CO.β-Dap.SC.T(ol)	**35**	1.6	0.51
13-CH_2CO.β-Dap.KC.T(ol)	**34**	0.35 (234)	0.65 (>1000)
13-CH_2CO.β-Dap.GC.T(ol)	**33**	-	0.22 (3.92)
13-CH_2CO.β-Dap.KC.amide	**32**	-	0.50 (0.02)
13-CH_2CO.SKC.amide	**31**	-	0.27 (12.6)
13-CH_2CO.GGCR.amide	**30**	-	6.2 (0.12)
13-CH_2CO.TGGC.amide	**29**	1.6 (>1000)	3.7 (>1000)
13-CH_2CO.GGCH.amide	**28**	-	8.2 (>1000)
octreotide	**2**	1.1	

blood, and tissue samples were collected and counted for radioactivity at 90 min postinjection. In addition, depreotide (**40**) and another peptide containing the compound **10** pharmacophore (**41**) that were described previously[17] were screened. The results are presented in Table 6.

The peptide with the best biodistribution results **39** was radiolabeled with Re-188 and its *in vivo* biodistribution in AR42J tumor xenograft mice compared to that of the corresponding Tc-99m complex. Results comparing Tc-99m (**39**) and Re-188 (**39**) at 4 and 24 h postinjection are shown in Table 7.

Results and Discussion

The synthetic protocol for the preparation of the peptides described herein was designed such that pharmacophore and chelator moieties could be prepared separately and subsequently conjugated via a sulfhydryl alkylation reaction involving a homocysteine residue or *N*-methylhomocysteine on the pharmacophore peptide and an N-terminal chloroacetyl contained on the chelator peptide. This convergent synthesis allowed for a straightforward approach for optimization of the final peptide: a separate initial optimization of the pharmacophore was conducted, and then SAR modification of the full peptide was effected by changes made on the small chelator peptides. The overall yields of the peptides ranged from ~25 to 52%, which was adequate to generate enough material (5−10 mg) for radiolabeling and biological screening.

The Tc-99m radiolabeling reactions utilized already well-established kit formulation chemistry[17] starting with pertechnetate $^{99m}TcO_4^-$ from a Mo-99/Tc-99m generator and employing stannous tin as a reductant and glucoheptonate as an exchange ligand. This radiolabeling method provides a robust, reliable method for radiolabeling cysteine-containing peptides with high radiochemical yields. The Re-188 radiolabeling procedure employed essentially the same formulation as the Tc-99m procedure except the starting radiochemical was perrhenate $^{188}ReO_4^-$ from a W-188/Re-188 generator, and ~20 fold more stannous tin was required to reduce the Re(VII) to Re(V). In addition, the Re-188 preparations were more prone to radiolytic decomposition owing to the β^- decay of the isotope, and therefore, anti-radiolytic stabilizers ascorbic acid and gentisate were added to the preparation postradiolabeling. The synthesis of the nonradioactive rhenium complexes of the peptides was also straightforward, prepared as previously described[17] from a Re(V) starting material $Bu_4N^+ReOBr_4^-$. The rhenium oxo

Table 6. Biodistribution of Tc-99m Complexes (average ± S.D.) in AR42J Rat Pancreatic Tumor Xenograft-bearing Nude Mice at 1.5 h Postinjection ($n = 6$)

	% ID/g			% ID			tumor ratios	
compd (no.)[a]	tumor	blood	kidneys	liver	G.I.	urine	T/K	T/B
13-CH_2C O.β-Dap. F(4-NH_2) .C.TS (**39**)	24.7 ± 1.3	0.8 ± 0.03	4.8 ± 0.5	7.7 ± 0.8	8.0 ± 0.7	59 ± 3	5.2	31
13-CH_2C O.β-Dap. F(4-NH_2) .C.T (**38**)	25.0 ± 3.4	0.4 ± 0.1	5.7 ± 0.9	4.9 ± 0.4	14 ± 0.5	53 ± 1	4.4	63
13-CH_2C O.β-Dap. F(4-NH_2) .C.T(ol) (**37**)	24.3 ± 5.4	0.4 ± 0.1	6.4 ± 1.1	3.7 ± 0.6	10 ± 1.6	47 ± 1	3.8	61
13-CH_2C O.β-Dap. YC.T(ol) (**36**)	27.6 ± 6.7	0.6 ± 0.2	7.7 ± 2.1	6.7 ± 0.5	22 ± 6	32 ± 13	3.6	46
13-CH_2C O.β-Dap. SC.T(ol) (**35**)	12.6 ± 1.3	0.2 ± 0.01	6.1 ± 0.8	2.5 ± 0.3	8.1 ± 0.5	59 ± 13	2.1	63
13-CH_2C O.β-Dap. KC.T(ol) (**34**)	10.2 ± 1.7	0.2 ± 0.01	26.8 ± 2.8	1.4 ± 0.8	3.1 ± 0.2	65 ± 4	0.4	51
13-CH_2C O.β-Dap. GC.T(ol) (**33**)	7.1 ± 1.0	0.5 ± 0.1	4.5 ± 0.8	6.6 ± 0.9	19 ± 3	43 ± 6	1.6	14
13-CH_2C O.β-Dap. KC.amid e (**32**)	7.5 ± 0.9	0.5 ± 0.2	42.5 ± 4.2	2.2 ± 0.6	3.2 ± 0.3	36 ± 5	0.2	15
13-CH_2C O.SKC.a mide (**31**)	10.3 ± 1.0	0.7 ± 0.1	41.9 ± 2.8	2.3 ± 1.0	5.2 ± 0.6	68 ± 9	0.2	15
13-CH_2C O.GGCR .amide (**30**)	7.2 ± 0.5	1.5 ± 0.03	32.3 ± 3.5	3.4 ± 0.8	7.9 ± 1.1	39 ± 5	0.2	5
13-CH_2C O.TGGC. amide (**29**)	3.8 ± 0.9	0.1 ± 0.02	4.7 ± 0.7	5.5 ± 0.4	30 ± 6	26 ± 4	0.8	38
13-CH_2C O.GGCH .amide (**28**)	0.8 ± 0.6	0.1 ± 0.01	3.0 ± 0.5	10.0 ± 2.0	42 ± 7	14 ± 2	0.3	8
11-CH_2C O.β-Dap. KC.T(ol) (**27**)	3.6 ± 1.3	0.4 ± 0.10	43.4 ± 2.9	2.0 ± 0.8	5.0 ± 1.2	51 ± 9	0.1	9
11-CH_2C O.β-Dap. KCK.ami de (**26**)	4.2 ± 0.4	0.2 ± 0.1	162 ± 3	6.2 ± 1.8	25 ± 0.2	12 ± 0.3	0.03	21
10-CH_2C O.β-Dap. KCK.ami de (**40**, depreotid e)	6.7 ± 0.3	0.6 ± 0.3	152 ± 9	5.9 ± 0.4	2.3 ± 0.4	8.9 ± 1.3	0.04	11
10-CH_2C O.GGCR .amide (**41**)	6.1 ± 1.0	1.3 ± 0.6	58 ± 6	5.7 ± 0.5	6.1 ± 1.4	15 ± 6	0.1	5

[a] Pharmacophore sequences are described in Table 1.

Table 7. Biodistribution of Tc-99m (**39**) and Re-188 (**39**) (average ± SD) in AR42J Rat Pancreatic Tumor Xenograft Mice at 4 and 24 h Postinjection ($n = 6$)

		% ID/g					% ID		
compd	time, h	tumor	blood	kidneys	spleen	pancreas	lung	liver	G.I.
Tc-99m (39)	4	27.5 ± 1.4	0.06 ± 0.00	5.4 ± 1.0	0.1 ± 0.0	7.5 ± 1.2	0.2 ± 0.1	3.3 ± 0.2	6.9 ± 1.2
Re-188 (39)	4	25.7 ± 7.6	0.26 ± 0.03	5.6 ± 1.4	1.1 ± 0.2	4.1 ± 0.9	0.2 ± 0.0	3.4 ± 0.2	7.2 ± 2.1
Tc-99m (39)	24	19.2 ± 4.1	0.02 ± 0.01	2.3 ± 0.3	0.1 ± 0.0	2.3 ± 0.4	0.05 ± 0.02	2.5 ± 0.4	1.9 ± 0.2
Re-188 (39)	24	18.2 ± 7.3	0.07 ± 0.01	2.4 ± 0.8	0.2 ± 0.1	1.2 ± 0.2	0.05 ± 0.00	1.2 ± 0.4	1.1 ± 0.1

product complexes were purified and isolated using standard preparative C18 HPLC methods and lyophilization as employed for the free peptides.

One of the main goals of this work was to improve upon the radiodiagnostic peptide depreotide to make it more suitable for radiotherapy. As an initial step to investigate how different positioning of the pharmacophore relative to the metallocomplex might effect the performance of the complexes, some modified pharmacophore peptides were evaluated for *in vitro* binding affinity to AR42J rat pancreatic tumor membranes (Table 4; Figure 4). The result was a pharmacophore that had improved binding affinity. Compound **10** is the pharmacophore for depreotide, which had a binding affinity (IC_{50}) of 1.5 nM. When the valine in **10** was substituted by threonine (compound **11**) and when the (N-Me)homocysteine and phenylalanine amino acid side chains were interchanged (compound **14**), improved (sub-nanomolar) binding affinity results were obtained (0.4 and 0.7 nM, respectively). When both of these changes to **10** were made (compound **13**), an optimized binding affinity of 0.1 nM was achieved. The positioning of the N-Me group (forming the cis peptide bond) on the amino acid adjacent to the Tyr residue in the cyclic peptide sequence appeared to be important to the high binding affinity, because when the N-Me substitutent in **13** was moved from the Hcy to the Phe group (compound **12**), the binding affinity of the pharmacophore decreased substantially, to 23.7 nM.

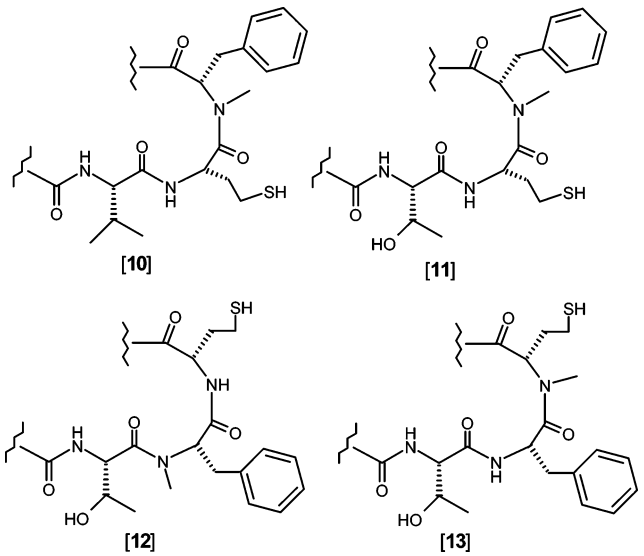

Figure 4. Sequence modifications in the pharmacophore optimization. Tyr-D-Trp-Lys omitted from peptide structures to simplify depiction of key features.

Several of the peptides and rhenium complexes of the peptides were screened *in vitro* for binding affinity to NCI-H69 human SCLC tumor membranes (Table 5). All of the ReO compounds exhibited good binding affinities (IC_{50}) to SSTR on the NCI-H69 tumor membranes in the low nanomolar to sub-nanomolar range. The exceptions were complexes of **28**, **29**, and **30**, with IC_{50} values in the mid-nanomolar range (3.7−8.2 nM). The metal centers of these compounds (Figure 3) consisted of either anionic complexes derived from triamde thiol chelate (compounds **28**−**31**, **41**) or neutral complexes derived from diamide amine thiol donor atoms (compounds **26**, **27**, **32**−**39**, **40**).[17] The exceptional (poorer binding) compounds all had triamide thiol chelators and therefore possessed a negative charge on the metal complex, which is consistent with previous results indicating that negative charge can be deleterious to the SSTR binding of these peptides.[17] In general the binding affinities of the peptides and ReO complexes were quite high, with values equivalent or better than octreotide (**2**). Binding affinities of this magnitude were expected to be well-suited for targeting SSTRs with a radiotherapeutic peptide and allowed us to proceed with further optimizing the peptides using biodistribution experiments. In comparing the results for the rhenium complexes vs the free

peptides, there is not as pronounced a trend toward improved binding upon metal complexation, as was observed previously for these types of SSTR analogues.[17]

Due to the similarity in atomic sizes and coordination chemistries of technetium and rhenium,[18] it is widely accepted that the chemical and physical properties of their metal complexes will correlate. Hence, the two metals have been used as surrogates for each other when it is necessary or convenient. For example, nonradioactive macroscopic rhenium complexes have been made in order to help characterize tracer Tc-99m radiopharmaceuticals.[35] In this case, the nonradioactive rhenium is more environmentally friendly, safer to work with, and free of radioactive waste storage/disposal issues as compared to the radioactive macroscopic technetium alternative: Tc-99g. Furthermore, it is also accepted that technetium and rhenium complexes of the same ligand ought to have similar biological properties. Therefore, nonradioactive rhenium complexes are used to evaluate *in vitro* binding properties of Tc-99m complexes,[17] and recently, fluorescent nonradioactive rhenium compounds have been proposed to assess the *ex vivo* subcellular distribution of the equivalent Tc-99m tracers.[36] In this work, we have chosen to use Tc-99m instead of Re-188 complexes in biodistribution screening studies for optimization of the SSTR-binding peptides for radiotherapy. Tc-99m is more readily available and less radiotoxic than Re-188, and its radiolabeling chemistry is more robust. Due to the expected similarities in the biological properties of technetium and rhenium complexes, we presumed that a peptide optimized using Tc-99m radiolabeled test compounds ought to also be optimized for the Re-188.

Biodistribution results for the Tc-99m peptides in AR42J rat pancreatic tumor xenograft nude mice are given in Table 6. Tc-99m depreotide (**33**) demonstrated good tumor uptake (6.8 %ID/g), but had high uptake in the kidneys (151.8 %ID/g), and relatively low urinary clearance (15 %ID). Such a distribution would predict high doses of radioactivity to nontarget organs and is consistent with the tumor regression study results for Re-188 depreotide.[23] The *in vitro* results for the pharmacophores (*vide supra*) had indicated that **11** has a better binding affinity for SSTR than the depreotide pharmacophore **10**. However, in one pair of peptides allowing a direct *in vivo* comparison of the pharmacophores, biodistribution results showed that the pharmacophore **11**-containing peptide **26** exhibited less tumor uptake than the corresponding pharmacophore **10**-containing peptide **40**. This is probably a reflection of the fact that biodistribution and tumor uptake is influenced by several factors other than binding affinity (for example, receptor-peptide internalization and bioavailability). In comparing pharmacophore **13**-containing peptides to analogues containing pharmacophores **10** or **11**, the biodistribution results were consistent with the *in vitro* result that **13** is the optimal pharmacophore. Hence, in cases where direct comparisons are possible, peptides containing pharmacophore **13** had the higher tumor uptake results (compare **30** vs **41**, and **34** vs **27**).

The depreotide peptide (**40**) and its pharmacophore **11**-containing analogue bearing the β-Dap.KCK.amide chelator/C-terminus (**26**) both had extremely high kidney uptake. The other peptide containing pharmacophore **11** (**27**) had tumor uptake and biodistribution similar to **26**, but with substantially less kidney retention. We note that because **27** has deleted Lys, it has less positive charge on the complex than **26** and depreotide. Similar Lys transformations to lower positive charge are known to lower kidney retention in radiolabeled peptides[37] and proteins.[38] In fact, the charge on the Tc-99m peptide complexes at the chelator appears to have had a major influence on the tumor and kidney uptake. Considering first the peptides with triamide thiol chelators, compounds **28** and **29** have a negative charge at the metal center owing to their GGC metal complex, and these peptides exhibited very low uptake in both the kidneys (3.0 and 4.7 %ID/g, respectively) and the tumor (0.8 and 3.8 %ID/g, respectively). The low kidney result is consistent with previous reports that indicated lower kidney uptake was associated with increased negative charge on a peptide complex.[39] The low tumor result may reflect the less-favorable binding affinities of these compounds (*vide supra*). Addition of a positive charge to the triamide thiol metal center by substituting Arg (**30** or **41**) or Lys (**31**) into the chelator increased the tumor uptake somewhat, but also increased the kidney uptake substantially (from 3 to 5 %ID/g to 32−58 %ID/g). Compound **31** had a reasonably good tumor uptake (10.3 %ID/g), but its kidney retention was unacceptably high (42 %ID/g). This apparent tradeoff between improved tumor uptake at the expense of worse kidney uptake effectively ruled out the triamide thiol type of chelators for these peptides.

Considering peptides with neutral diamide amine thiol chelators, compound **32** is equivalent to depreotide, except the pharmacophore is **13** (instead of **10**), and C-terminal lysine has been deleted. This peptide exhibited considerably less kidney uptake than depreotide (43 vs 152 %ID/g), slightly higher tumor uptake (7.5 vs 6.8 %ID/g), and better urinary clearance (36 vs 15 %ID). Again, we observed that removing a Lys from the peptide decreases kidney uptake substantially. Replacing the C-terminal amide NH_2 by Thr(ol) (**34**) improved the tumor uptake still further to 10.2 %ID/g, decreased the kidney still further to 26.8 %ID/g, and increased the urinary clearance considerably to 65 %ID. To lower the kidney uptake still further (to <7 %ID/g), substitutions of the Lys residue in the chelator by neutral amino acids were made (Gly for Lys: **33** and Ser for Lys: **35**), making the metal center neutral. The Gly substitution (peptide **33**) resulted in worse tumor uptake (7.1 vs 10.2 %ID/g), but the Ser-substitution resulted in a peptide **35** with improved tumor uptake (12.6 %ID/g). Hence, peptide **35** had tumor uptake and biodistribution behavior that was considerably better than depreotide, particularly in regard to tumor uptake, kidney uptake, and urinary excretion. This compound was the first in this class of peptides that had a tumor:kidney ratio >2.

When **35** was modified to incorporate Tyr instead of the Ser in the chelator (**36**) a further dramatic increase in tumor uptake was observed (from 12.6 to 27.6 %ID/g). Other results indicated that the critical feature leading to this improved tumor uptake was placement of an aromatic substituent at this amino acid position in the chelator. The percent injected dose per gram in the AR42J tumors more than doubled with this substitution, and relative to depreotide, the tumor uptake was now increased 4-fold. Incorporation of the aromatic substituent also increased the liver and G.I. retention and decreased the urinary excretion of the peptide (a result of increased peptide lipophilicity effected by the aromatic moiety), so further modifications were aimed at readjusting the biodistribution. Replacement of the phenolic OH group of the tyrosine with a *p*-NH_2 group (**37** vs **36**) resulted in decreased liver and G.I. uptake and increased urinary excretion. Finally, changing the C-terminus to a carboxyl functionality instead of an amide (**38**), and addition of a Ser amino acid, resulted in the peptide **39**, with high tumor uptake, the highest tumor:kidney ratio, and good urinary clearance. Relative to depreotide, the new clinical candidate peptide **39** has dramatically improved tumor uptake (25 %ID/g vs 7 %ID/

g), 30-fold decreased kidney retention (5 %ID/g vs 152 %ID/g), and substantially increased urinary clearance (59 %ID vs 15 %ID).

A biodistribution study was done with Tc-99m (**39**) and Re-188 (**39**) in AR42J mice at 4 and 24 h timepoints to compare the technetium and rhenium complexes in the *in vivo* animal model as well as to evaluate the biodistribution beyond 1.5 h. The results (Table 7) show quite clearly that the biological properties of the Re-188 compound are nearly identical to the Tc-99m compound. The one exception is the pancreas, where uptake is higher for the Tc-99m analogue vs the Re-188 analogue (7.5 vs 4.1% ID/g at 4 h). By 24 h, the pancreas results have dropped to comparable levels (2.3 vs 1.2% ID/g). There is also a slight increase in hepatobiliary uptake/clearance for the Tc-99m peptide relative to the Re-188 peptide at the later timepoint, and the Tc-99m analogue has lower blood and spleen values at the earlier timepoint, but all the values are quite low and therefore essentially the same. These results confirm the equivalence of the Tc-99m and Re-188 in this animal model and justify our decision to use Tc-99m complexes to optimize the Re-188 peptide. The later timepoint results also demonstrate that the radiolabeled peptide is retained in the tumor for long periods (>18 %ID/g) at 24 h and therefore is well-suited for radiotherapy.

Conclusions

A promising peptide agent for radiotherapy of SSTR-expressing tumors has been developed: **39**. The cyclic somatostatin analogue peptides comprising hexapeptide pharmacophores and metal chelator amino acid sequences that were originally designed for complexing Tc-99m in the commercial radiodiagnostic agent Tc-99m depreotide have been adapted for radiotherapy with β^--emitting rhenium isotopes. Pharmacophore peptides were optimized by testing derivatives for *in vitro* binding affinity to AR42J rat pancreatic tumor cell membranes. Subsequently peptides with chelating domains and their oxorhenium complexes were tested for *in vitro* binding to NCI H69 human SCLC tumor membranes, and low- to sub-nanomolar binding (IC_{50}) was observed. Final optimization of the peptide agent was accomplished through *in vivo* biodistribution studies in AR42J tumor xenograft mice using Tc-99m radiolabeled complexes. The biological equivalence of the technetium and rhenium compounds was subsequently confirmed in comparison biodistribution studies of the Re-188 vs Tc-99m (**39**). The charge on the metal complex appeared to have an important influence on the biological properties of the agents, particularly the tumor and kidney uptake. Peptides possessing neutral N_3S diamide amine thiol chelators appeared to have better biological properties relative to negatively charged triamide thiol chelators. Substituting an aromatic amino acid into the diamide amine thiol chelator β-Dap-X-Cys had a profoundly beneficial effect on (approximately doubled) the tumor uptake of the peptides. Radiolabeled **39** has dramatically improved tumor uptake, substantially lower kidney retention, and increased urinary clearance relative to the commercial radiodiagnostic agent Tc-99m depreotide. It also has prolonged retention in the tumor, and is well-suited for radiotherapy of solid tumors. The Re-188 complex of **39** was selected for evaluation in clinical studies for treatment of lung cancer.

Experimental Section

Symbols and abbreviations generally follow the IUPAC-IUB recommendations as published in *Int. J. Pept. Protein Res.* (**1984**, *24*, 9−37). Amino acids were of the L-configuration unless stated otherwise. All protected amino acids used were purchased from Bachem, Novabiochem, or Advanced Chemtech and used as is. Rhenium oxo complexes of the peptides were prepared as described previously.[17] Other chemicals and solvents were purchased from either Aldrich, Perseptive Biosystems, Applied Biosystems, EM Science, Burdick and Jackson, Fluka, or VWR Scientific and used as is. Aldrich SureSeal solvents were used when anhydrous conditions were necessary. When indicated, an automated Applied Biosystems 431A peptide synthesizer was used. For manual peptide synthesis, the reaction vessel used was purchased from Safe-Lab, Santee, CA. Analytical HPLC measurements were made on a Waters system using a Vydac C18 column, 5 micron particle size, 300 Å pore size, 4.6 × 250 mm at a flow rate 1.2 mL/min, and with 0.1% TFA mobile phases in acetonitrile/water. Preparative HPLC was performed on a Waters LC-4000 system using a 4 × 32.5 cm C18 Delta Pak preparative HPLC column with the same (TFA) mobile phases as described above for the analytical runs. Fast atom bombardment mass spectra (FABMS) were obtained by M-Scan using a VG Analytical ZAB 2-SE instrument.

After amino acid coupling, quantitative analysis via a ninhydrin test was performed as follows: A 3−10 mg sample of resin was placed in a test tube. A phenol/ethanol (76:24) solution (75 μL) was added to the resin sample followed by the addition of 0.2 mM KCN/pyridine (100 μL) and 0.28 M ninhydrin in ethanol (75 μL). The tubes were heated at 100 °C for 5 min and diluted with 4.80 mL of ethanol/water (60:40). The color of the resulting solution was observed visually. If the color of the solution was blue, unreacted free amine was present, indicating that the coupling reaction was not completed.

L-Phenylalanyl-*N*-methyl-*S*-trityl-L-homocysteinyl-*O*-*tert*-butyl-L-tyrosinyl-N^{in}-Boc-D-tryptophanyl-*N*-ϵ-Boc-L-lysinyl-*O*-*tert*-butyl-L-threonine (protected linear peptide). *O*-*tert*-Butyl-L-threonine supported on 2-chlorotrityl resin (9.09 g, 1.1 mmol/g, 10 mmol) was sequentially coupled to *N*-α-Fmoc-*N*-ϵ-Boc-L-lysine, *N*-α-Fmoc-N^{in}-Boc-D-tryptophan, *N*-Fmoc-*O*-*tert*-butyl-L-tyrosine, and *N*-Fmoc-*N*-methyl-*S*-trityl-L-homocysteine using the following solid-phase peptide synthesis protocol: In a manual peptide synthesis vessel, the resin supported threonine was washed with NMP (25 mL, 3 × 1 min) with agitation by bubbling with argon gas. The final NMP wash was drained from the resin. Separately, *N*-α-Fmoc-*N*-ϵ-Boc-L-lysine (11.7 g, 25 mmol), HATU reagent (9.51 g, 25 mmol), and HOAt (3.40 g, 25 mmol) were dissolved in NMP (70 mL). Diisopropylethylamine (8.7 mL, 50 mmol) was added to the amino acid solution followed by swirling for 2 min. The resulting activated amino acid solution was added to the vessel containing the resin-supported N-terminal free amine. The resin was agitated by bubbling with argon gas for 2 h followed by draining away the reaction solution. The resin was washed with DMF (75 mL, three times), dichloromethane (75 mL, three times), and DMF (75 mL, three times). The completeness of coupling reaction was determined by qualitative ninhydrin analysis on a small sample of resin. If the ninhydrin analysis indicated that the coupling was incomplete, the resin was reacted with activated amino acid precursor once more on a half-scale for 2 h. Once ninhydrin analysis indicated the coupling to be complete, the N-terminal Fmoc group was then removed by treating the resin with 5% piperidine in 1:1 (v/v) NMP/DCM (75 mL) for 10 min, followed by treatment with 20% piperidine/NMP (75 mL) for 15 min. The resin was subsequently washed with DMF (75 mL, three times) and DCM (75 mL, three times).

As performed above, in four sequential procedures, *N*-α-Fmoc-N^{in}-Boc-D-tryptophan (13.2 g, 25 mmol then 6.6 g, 12.5 mmol), *N*-Fmoc-*O*-*tert*-butyl-L-tyrosine (11.5 g, 25 mmol then 5.75 g, 12.5 mmol), *N*-Fmoc-*N*-methyl-*S*-trityl-L-homocysteine (15.0 g, 25 mmol then 7.5 g, 12.5 mmol), and *N*-Fmoc-phenylalanine (9.7 g, 25 mmol) were similarly reacted with the resin-supported peptide followed by Fmoc group removal to produce l-phenylalanyl-*N*-methyl-*S*-trityl-L-homocysteinyl-*O*-*tert*-butyl-L-tyrosinyl-N^{in}-Boc-D-tryptophanyl-*N*-ϵ-Boc-L-lysinyl-*O*-*tert*-butyl-L-threonine-2-chlorotrityl resin. The coupling of the last amino acid (Phe) was monitored by HPLC rather than ninhydrin analysis with a small-scale cleavage from the

resin to generate the HPLC sample as follows: a small portion of resin (approximately 20−40 beads) was treated with 1:4 (v/v) hexafluoro-2-propanol/DCM (200 μL) for 5 min to affect cleavage of the protected peptide from the resin. A portion of this cleavage mixture (15 μL) was diluted with 0.1% TFA (v/v) in 90:10 (v/v) acetonitrile water (150 μL) and examined by HPLC analysis. Solvent A = 0.1% TFA in water; Solvent B = 0.1% TFA in 90/10 ACN/water. Gradient = 50−100% B over 20 min (product retention time = 19.9 min).

The resin-supported peptide was treated with 1:4 (v/v) hexafluoro-2-propanol/DCM (75 mL, 2 × 10 min) with subsequent collection of the cleavage solution into a 1000 mL round-bottom flask. The resin was washed with DCM (75 mL, 4 × 5 min), adding each wash to the round-bottom containing the cleavage solution. The volatiles were removed on a rotory evaporator *in vacuo* to yield protected linear hexapeptide. Some of the material was dissolved in Solvent B and analyzed by HPLC using the same procedure as described above (product retention time = 19.9 min).

cyclo-[L-Phenylalanyl-*N*-methyl-L-homocysteinyl-L-tyrosinyl-D-tryptophanyl-L-lysinyl-L-threoninyl] (13). The linear protected hexapeptide was dissolved in anhydrous DMF (400 mL) in a dry 1000 mL round-bottom flask under an atmosphere of argon. To this solution was added diisopropylethylamine (1.75 mL, 10 mmol) followed by the addition of HATU reagent (3.8 g, 10 mmol). The reaction mixture was stirred under an atmosphere of argon for 1.5 h, at which time HPLC analysis (same method as described above) indicated that the cyclization was complete (cyclic protected peptide retention time = 23.55 min). A solution of 1% (v/v) TFA in H_2O (80 mL) was added, and the reaction mixture was concentrated *in vacuo* to dryness in a rotory evaporator under high vacuum. After drying, the crude peptide was treated with DCM (120 mL), and the resulting suspension was allowed to stand for 0.5 h. The solution was filtered through a scintered glass funnel and the solid in the funnel washed with additional DCM (20 mL). The combined DCM solutions were treated with triisopropylsilane (3.0 mL) and ethanedithiol (3.0 mL), followed by the addition of a mixture of 95:5 (v/v) TFA/H_2O (140 mL). The deprotection solution was allowed to stand for 1 h, and the volatiles were removed *in vacuo* on a rotory evaporator under high vacuum. The residue was dissolved in 0.1% TFA (v/v) in 90:10 (v/v) acetonitrile/water (Solvent B, 100 mL) and diluted with 0.1% TFA (v/v) in water (Solvent A, 300 mL). The resulting cloudy suspension was allowed to stand for 15 min and filtered through a pad of Celite. The Celite pad was washed with a 3:1 mixture of Solvent A/Solvent B and the wash combined with the filtrate recovered previously. Crude **13** product was analyzed by HPLC using the same HPLC method as described above, except with a 20−50% B gradient over 20 min (retention time = 16.5 min).

The product was purified by preparative reversed-phase HPLC as follows: The solution of crude product was divided into three equal portions of about 150 mL and each separately applied to a preparative C18 HPLC column which had been equilibrated in Solvent A. The column was eluted at 75 mL/min. with a linear gradient of 100:0 to 72:28 A/B over 10 min and kept at 72:28 A/B for 10 min. This was followed by a 72:28 to 67:33 A/B gradient over 35 min. Fractions were collected and analyzed by HPLC using the same HPLC method as described above, except with a 30−35% B gradient over 20 min (retention time = 15.4 min). Fractions containing **13** product with a purity of >95% were pooled. Fractions containing product with a purity of 50% to 95% were repurified by conditions identical to that above and pure fractions from the repurification were combined with the pure fractions from the initial chromatography. Acetonitrile was removed from the final pool of pure product by evaporation *in vacuo* on a rotory evaporator, and the resulting aqueous solution was frozen and lyophilized. The yield of **13** after lyophilization was 1.1 g. Analytical HPLC of the final (**13**) material showed purity >96%. The **13** pharmacophore peptide was also confirmed by electrospray mass spectrometry.

***N*-β-Chloroacetyl-*N*-α-Boc-L-diaminopropionyl-L-4-Boc-aminophenylalanyl-*S*-trityl-L-cysteinyl-*O*-*tert*-butyl-L-threonyl-*O*-*tert*-butyl-L-serinyl-2-chlorotrityl Resin.** *O*-*tert*-Butyl-L-serine supported on 2-chlorotrityl resin (7.2 g, 1.0 mmol/g, 7.2 mmol) was sequentially coupled to *N*-Fmoc-*O*-*tert*-butyl-L-threonine, *N*-Fmoc-*S*-trityl-L-cysteine, *N*-α-Fmoc-L-4-Boc-aminophenylalanine, *N*-α-Boc-*N*-β-Fmoc-L-diaminopropionic acid, and chloroacetic acid using the following solid-phase peptide synthesis protocol (DIC was used for coupling cysteine and diaminopropionic acid instead of HBTU reagent[40]): In a manual peptide synthesis vessel the resin-supported serine was washed with NMP (75 mL, 3 × 1 min) with agitation by bubbling with argon gas. The final NMP wash was drained from the resin. Separately, *N*-Fmoc-*O*-*tert*-butyl-L-threonine (7.16 g, 18 mmol) was dissolved in NMP (20 mL), and to this solution was added a 1:1 mixture of HBTU reagent and HOBt in DMF (0.45 M, 39.6 mL, 18 mmol), followed by the addition of diisopropylethylamine (6.3 mL, 36 mmol). The resulting activated amino acid solution was swirled for 2 min and added to the vessel containing the resin-supported N-terminal free amine. The resin was agitated by bubbling with argon gas for 2 h followed by draining away the reaction solution. The resin was washed with DMF (75 mL, three times), dichloromethane (75 mL, three times), and DMF (75 mL, three times). The completeness of coupling reaction was determined by qualitative ninhydrin analysis on a small sample of resin. If the ninhydrin analysis indicated that the coupling was incomplete, the resin was reacted with activated amino acid precursor once more for 2 h. Once ninhydrin analysis indicated the coupling to be complete, the N-terminal Fmoc group was then removed by treating the resin with 5% piperidine in 1:1 (v/v) NMP/DCM (75 mL) for 10 min, followed by treatment with 20% piperidine/NMP (75 mL) for 15 min. The resin was subsequently washed with DMF (75 mL, three times) and DCM (75 mL, three times).

The conditions for the couplings with *N*-Fmoc-*S*-trityl-L-cysteine and *N*-α-Boc-*N*-β-Fmoc-L-diaminopropionic acid were identical to those describe above except diisopropylcarbodiimide (2.8 mL, 18 mmol) and HOBt (2.43 g, 18 mmol) was used instead of HBTU reagent and diisopropylethylamine. As performed above, in four sequential procedures *N*-Fmoc-*S*-trityl-L-cysteine (10.54 g, 18 mmol), *N*-α-Fmoc-L-4-Boc-aminophenylalanine (5.03 g, 10 mmol), and *N*-α-Boc-*N*-β-Fmoc-L-diaminopropionic acid (4.27 g, 10 mmol) were similarly reacted with the resin-supported peptide followed by Fmoc group removal to produce *N*-α-Boc-L-diaminopropionyl-4-Boc-amino-L-phenylalanyl-*S*-trityl-L-cysteinyl-*O*-*tert*-butyl-L-threonyl-*O*-*tert*-butyl-L-serinyl-2-chlorotrityl resin. The β-amino of the N-terminal diaminopropionic acid residue was reacted with chloroacetic acid (1.70 g, 18 mmol) using HBTU reagent and DIEA as described above for threonine and 4-aminophenylalanine to produce *N*-β-Chloroacetyl-*N*-α-Boc-L-diaminopropionyl-4-Boc-amino-L-phenylalanyl-*S*-trityl-L-cysteinyl-*O*-*tert*-butyl-L-threonyl-*O*-*tert*-butyl-L-serinyl-2-chlorotrityl resin. This intermediate was examined by HPLC analysis using the 50−100% B gradient as follows: a small portion of resin (approximately 20−40 beads) was treated with 1:4 (v/v) hexafluoro-2-propanol/DCM (200 μL) for 5 min to affect cleavage of the protected peptide from the resin. A portion of this cleavage mixture (15 μL) was diluted with 0.1% TFA (v/v) in 90:10 (v/v) acetonitrile water (150 μL) and examined by HPLC analysis. (retention time = 21.10 min).

***N*-β-Chloroacetyl-L-diaminopropionyl-4-amino-L-phenylalanyl-*S*-trityl-L-cysteinyl-L-threonyl-L-serine (25).** Resin-supported peptide *N*-β-Chloroacetyl-*N*-α-Boc-L-diaminopropionyl-L-4-Boc-aminophenylalanyl-*S*-trityl-L-cysteinyl-*O*-*tert*-butyl-L-threonyl-*O*-*tert*-butyl-L-serinyl-2-chlorotrityl resin was treated with 95:5 (v/v) TFA/H_2O (100 mL) for 1.5 h. The volatiles were removed on a rotory evaporator, the residue was treated with chloroform (100 mL), and the chloroform then removed on a rotory evaporator. The treatment with chloroform was repeated several times until the yellow/orange color of the solution and residue disappeared. Disappearance of the yellow/orange color is indicative of the loss of the trityl carbocation and reattachment of the trityl group to the cysteine side-chain sulfhydryl. **25** was purified by preparative reversed-phase HPLC as follows: Crude product was dissolved in 0.1% TFA (v/v) in 1:1 (v/v) CH_3CN/H_2O and divided into two equal portions. Each portion was separately diluted with 0.1% (v/

v) TFA/H_2O (Solvent A) and loaded onto a preparative C18 HPLC column which had been equilibrated in Solvent A. The column was eluted at 75 mL/min. with Solvent A for 5 min, a 2:8 mixture of Solvent B/Solvent A for 8 min (Solvent *B* = 0.1% TFA (v/v) in 90:10 (v/v) CH_3CN/H_2O), a 3:7 mixture of Solvent B/Solvent A for 15 min, followed by a flush with Solvent B for 10 min. The effluent was monitored by UV at 240 nm, and fractions were collected and analyzed by HPLC using the same conditions as described above except with a 20−50% B gradient. Fractions containing **25** product with a purity of >90% were pooled. Acetonitrile was removed from the final pool of pure product by evaporation *in vacuo* on a rotory evaporator, and the resulting aqueous solution was frozen and lyophilized. The yield of chloroacetylated peptide **25** was 2.0 g. An analytical HPLC of this intermediate showed purity >98% (product retention time = 17.94 min). The mass of the peptide was confirmed by electrospray mass spectrometry.

cyclo-[L-Phenylalanyl-*S*-(acetyl-L-diaminopropionyl-L-4-aminophenylalanyl-L-cysteinyl-L-threonyl-L-serine)-*N*-methyl-L-homocysteinyl-L-tyrosinyl-D-tryptophanyl-L-lysinyl-L-threoninyl] (39). A 0.15 M carbonate buffer was prepared as follows: Sodium hydrogen carbonate (12.6 g) was dissolved in deionized water (900 mL), and to this solution was added 0.1 M EDTA, disodium salt (10 mL). Addition of 1.0 M NaOH to the solution above was then carried out until a pH of 10.00 was reached. Separately, **13** trifluroroacetate (1.00 g, 1.03 mmol) and **25** ditrifluoroacetate (1.22 g, 1.10 mmol) were combined in a 1000 mL round-bottom flask, and the atmosphere was purged with argon gas. To the solids were added argon-sparged acetonitrile (100 mL) and argon-sparged 0.15 M carbonate buffer (pH = 10.0, 100 mL). The progress of the reaction was monitored by HPLC using the 20−50% B gradient (retention time of **39**(Trt) = 20.4 min, retention time of **13** = 18.7 min, retention time of **25** = 19.0 min). After 24 h, 1.0% (v/v) TFA in H_2O was added to the reaction mixture and the volume of the solution was reduced to about half volume by evaporation *in vacuo* on a rotory evaporator. The remaining aqueous solution was frozen and lyophilized to yield a white solid (5.35 g).

Crude **39**(Trt) (5.32 g) was placed in a 1000 mL round-bottom flask equipped with a magnetic stir bar. Triisopropylsilane (2.5 mL) was added followed by the addition of 1:1 (v/v) TFA/DCM (125 mL). The reaction mixture was stirred for 30 min, and the volatiles were removed *in vacuo* on a rotory evaporator. The residue was dissolved in 0.1% (v/v) TFA in 90:10 (v/v) acetonitrile/water (Solvent B, 50 mL), and the solution was diluted with 0.1% TFA (v/v) in water (Solvent A, 450 mL). The resulting suspension was filtered through a pad of Celite (prepared in 9:1 Solvent A/Solvent B), and the Celite pad was washed with 9:1 Solvent A/Solvent B (2 × 100 mL). Crude **39** product was analyzed by HPLC also with the 20−50% B gradient (retention time = 13.8 min).

The product was purified by preparative reversed-phase HPLC as follows: The combined filtrate and washes were applied to a preparative C18 HPLC column which had been equilibrated in 90:10 Solvent A/Solvent B. The column was eluted at 75 mL/min with a linear gradient of 90:10 to 85:15 A/B for 5 min followed by a gradient of 85:15 A/B to 77:23 A/B over 40 min. Fractions were collected and analyzed by HPLC using a 20−25% B over 20 min gradient. Fractions containing product with a purity of >95% were pooled, and acetonitrile was removed from the final pool of purified product by evaporation *in vacuo* on a rotory evaporator. The resulting aqueous solution was frozen and lyophilized. The yield of **39** was 1.30 g. An analytical HPLC of the final product showd purity >97%. The mass of **39** was confirmed by electrospray mass spectrometry.

Tc-99m Radiolabeled Peptides. Tc-99m pertechnetate TcO_4^- was obtained from a commercial Mo-99/Tc-99m generator (Dupont). "Placebo" kits were prepared containing all components (lyophilized) necessary to radiolabel with Tc-99m except the peptides in a 5 mL vial, stoppered under nitrogen. The placebo kit vials contained 5 mg of sodium α-D-glucoheptonate dihydrate, 100 of μg edetate disodium (EDTA), and 50 of μg tin(II) chloride dihydrate at pH 7.4. Peptides to be radiolabeled were dissolved in normal saline at 1 mg/mL, and 100 μg (100 μL) of peptide was added to placebo kits. Vials were reconstituted with normal saline/generator eluate totaling 1.0 mL containing 25−50 mCi $^{99m}TcO_4^-$ and heated for 10 min in a boiling water bath. After cooling the vials at room-temperature for ≥10 min, the Tc-99m complexes were tested for radiochemical purity (RCP) by thin-layer chromatography (TLC) and analytical reversed phase HPLC.

TLC was done on ITLC SG strips (Gelman) and developed in saturated NaCl/saline (SAS), 1:1 methanol:1 M ammonium acetate in water (MAM), and methyl ethyl ketone (MEK). In the SAS TLC system, Tc-99m peptide and Tc-99m nonmobile impurities remain at the origin, while in the MAM TLC system, only Tc-99m nonmobiles remain at the origin. In the MEK system, all Tc-99m species except Tc-99m pertechnetate remain at the origin. TLC RCP (% Tc-99m peptide) was calculated as (% origin SAS) − (% origin MAM), and % Tc-99m pertechnetate was calculated as % solvent front MEK. In all cases, the TLC RCP was greater than 95%.

RCP of the Tc-99m peptides was also determined by analytical reversed phase HPLC on a Zorbax 300SB C18 column (Agilent, 5 μm, 4.6 × 250 mm) with 0.1% trifluoroacetic acid in acetonitrile/water. The flow rate was 1.2 mL/min, and detection was radiometric. A typical HPLC gradient was 20−50% B over 20 min, where A = 0.1% TFA in water, B = 0.1% TFA in 90/10 acetonitrile/water. Gradients were adjusted such that the Tc-99m peptide species eluted at retention time = 10−20 min (20 min gradient). HPLC RCP was calculated as the % area of the main Tc-99m peptide peak(s). In all cases, the HPLC RCP was greater than 85%.

Re-188 (39). Re-188 perrhenate ReO_4^- was obtained from a W-188/Re-188 generator (Oak Ridge National Labs). The placebo kit described above for Tc-99m radiolabeling was also used for the Re-188 radiolabeling, and additional stannous tin was used. Therefore, 100 μg (100 μL) of peptide in saline was added to a placebo kit, followed by 1200 μg of $SnCl_2 \cdot 2H_2O$ as 120 μL of a 10 mg/mL solution in ethanol (used immediately after dissolution). The vial was reconstituted with normal saline/generator eluate totaling 1.5 mL containing 30 mCi $^{188}ReO_4^-$ and heated for 15 min in a boiling water bath. After cooling the vials at room-temperature for ≥10 min, a second vial containing freeze-dried ascorbic acid (10 mg) and sodium gentisate monohydrate (20 mg) radiolytic stabilizers was reconstituted with 2 mL of saline, and the entire volume was added to the first vial containing the radiolabeled peptides. The Re-188 (**39**) was tested for radiochemical purity (RCP) by thin-layer chromatography (TLC) using the same methods as described above for the Tc-99m peptides and by a similar analytical reversed phase HPLC method utilizing a 50−54% B gradient over 25 min.

Pharmacophore Binding Affinity. [^{125}I]Somatostatin-14 ([^{125}I]-SRIF-14) was obtained from Amersham. Unlabeled SRIF-14 was purchased either from Bachem or from Sigma. Protease inhibitors, leupeptin, aprotinin, bacitracin, and benzamidine and other reagents were obtained from Sigma. Protease inhibitors were prepared in DMSO at a concentration 500× higher than the final assay concentration. The prepared protease solution was stored at −20 °C and diluted with buffer solution before use.

Membrane preparations used in these studies were prepared from two commercially available tumor cell lines, the human small cell lung cancer line NCI-H69, and the rat pancreatic tumor cell line AR42J, obtained from American Type Culture Collection (ATCC). NCI-H69 cells were maintained by serial passage in RPM1 1640 with 10% fetal calf serum. Cells in culture flasks were incubated at 37 °C with 5% CO_2 in air atmosphere following recommendations from the supplier.

Cultured cells were first detached from plates with phosphate-buffered saline, pH 7.4, containing 2 mM EDTA, and centrifuged at 1500*g* for 10 min. Cells were then resuspended in 5−10 mL of the homogenization buffer (1 mM sodium bicarbonate, pH 7.4, 1 mM EDTA, 1 mM EGTA, 2.5 mM DTT, 5 μg/mL leupeptin, 5 μg/mL aprotinin, 100 μg/mL bacitracin, 100 μg/mL benzamidine) for 10 min on ice. The cells were lysed for 30 s twice in a polytron. The lysate was centrifuged at 1000*g* for 10 min at 4 °C. This step

was repeated twice with the homogenation buffer in the absence of protease inhibitors. The pellet was then resuspended at 1−5 mg membrane protein/mL in 25 mM Tris, pH 7.4, without the addition of protease inhibitors, and the membranes were stored at −80 °C before use. Membrane protein concentration was determined spectroscopically using bicinchonic acid (BCA) protein assay kit (Pierce Chemical Inc.).

All [^{125}I]SRIF-14 binding assays were performed in 0.5 mL of binding buffer containing 50 mM HEPES, pH 7.5, 10 mM $MgCl_2$, 0.25% BSA (w/v) containing protease inhibitors (same as above) and incubated at 37 °C for 45 min. After incubation, samples were kept at 4 °C and rapidly filtered under vacuum through a Whatman GF/B glass fiber filter with a 12-well harvester (Skatron Instruments Inc). The filter was washed for 9 s with cold 50 mM HEPES, pH 7.5, 10 mM $MgCl_2$, 0.25% BSA (w/v). Thirty five pmoles of [^{125}I]-SRIF-14 was used in each tube. Peptides were dissolved in DMSO and serially diluted with DMSO. Five microliters of peptide solution in DMSO was used to obtain the final concentration (0.01 nM to 100 nM). DMSO (5 μL) was added to the tube without any peptide or unlabeled somatostatin, so that each tube contained 1% DMSO. All compounds were tested in duplicate at five different concentrations.

The maximal specific binding was calculated by subtracting nonspecific binding from total binding in the absence of somatostatin. Nonspecific binding was defined as the binding of [^{125}I]-SRIF-14 which was not displaceable with an excess (1×10^{-6} M) of unlabeled somatostatin-14. The bound [^{125}I]SRIF-14 without excess unlabeled somatostatin-14 added was defined as total binding. The difference between total and nonspecific binding was defined as specific binding. The percent inhibition (% inh) was expressed as

$$\%\ \text{inh} = [(\text{total binding} - \text{total binding in the presence of peptide})/\text{specific binding}] \times 100\%$$

Inclusion of protease inhibitors in the homogenizing medium as well as assay buffer was essential to maintain the integrity of both [^{125}I]SRIF-14 and somatostatin analogues for the receptor binding assay and to obtain optimal specific binding. The highest specific binding was observed when $MgCl_2$ (10 mM) was included. Mamebranes were finally resuspended in a sodium-free medium, and receptor binding assays were performed in the absence of sodium ions.

The potency of the compounds in inhibiting the binding of [^{125}I]-SRIF-14 to isolated membranes was expressed as the IC_{50}, defined as the concentration of compound inhibiting 50% of the specific binding. Binding isotherms indicated that many compounds bound to two classes of receptors. IC_{50} values were calculated from the data by computerized nonlinear least-squares curve fitting program (GraphPad Prism) assuming two classes of receptor binding sites.

Biodistribution Studies. Rat panceatic AR42J cells (ATCC) were grown in Modified Ham's F12K medium (Sigma) containing 20% fetal bovine serum (FCS) (Sigma) under sterile conditions in 95% humidity and 5% CO_2. At a density of approximately 10×10^6 cells per T150 flask, the cells were harvested with trypsin and collected by centrifugation at 2400 rpm (800*g*) for 15 min in a benchtop centrifuge. The cells were resuspended in medium containing 20% FCS for implantation.

Six female nude mice (CrlLNU/NU-nuBR, 6−8 weeks old) were injected subcutaneously into the right flank with tumor cells (2×10^7/100 μL) in 20% matrigel (Collaborative Biomedical Products). Fourteen days after inoculation, tumors were visible in all animals. Three weeks after inoculation, tumors were aseptically dissected, minced, and implanted into 60 nude mice using a trochar. The tumor xenografts from the second passage were used for biodistribution studies.

A dose of approximately 50−100 μCi Tc-99m or Re-188 peptide/mouse was injected intravenously in a total volume of 100 μL. Mice were sacrificed 90 min, 4 h, or 24 h postinjection by decapitation, and the trunk blood was collected. Tumors (one to three per mouse), liver, lung, spleen, pancreas, gastrointestinal tract, kidneys, urine, and samples of muscle from both legs (quadriceps femoralis) were collected, weighed, and counted for radioactivity.

Supporting Information Available: Cyclic peptide pharmacophore MS results, chloroacetyl precursor MS results, and pharmacophore−chelator conjugate (final peptide) MS results. This material is available free of charge via the Internet at http://pubs.acs.org.

References

(1) Benali, N.; Ferjoux, G.; Puente, E.; Buscail, L.; Susini, C. Somatostatin receptors. *Digestion* **2000**, *62*, 27−32.

(2) (a) Hoyer, D.; Bell, G. I.; Berelowitz, M.; Epelbaum, J.; Feniuk, W.; Humphrey, P. P.; O'Carroll, A. M.; Patel, Y. C.; Schonbrunn, A.; Taylor, J. E.; Reisine, T. Classification and nomencalture of somatostatin receptors. *Trends Pharm. Sci.* **1995**, *16*, 86−88. (b) Patel, Y. C.; Srikant, D. B. Subtype selectivity of peptide analogues for all five cloned human somatostatin receptors (hsstr 1−5). *Endrocrinology* **1994**, *135*, 2814−17.

(3) (a) Reubi, J. C.; Krenning, E.; Lamberts, S. W.; Kvols, L. In vitro detection of somatostatin receptors in human tumors. *Digestion* **1993**, *54*(suppl. 1), 76−83. (b) Hansson, J.; Bjartel, A.; Gadaleanu, V.; Dizeyi, N.; Abrahamsson, P.-A. Expression of somatostatin receptor subtypes 2 and 4 in human benign prostatic hyperplasia and prostatic cancer. *The Prostate* **2002**, *53*, 50−59.

(4) (a) Reubi, J. C.; Horisberger, U.; Laissue, J. High density of somatostatin receptors in veins surrounding human cancer tissue: role in tumor-host interaction? *Int. J. Cancer* **1994**, *56*, 681−88. (b) Denzler, B.; Reubi, J. C. Expression of somatostatin receptors in peritumoral veins of human tumors. *Cancer* **1999**, *85*, 188−98.

(5) Stewart, P. M.; James, R. A. The future of somatostatin analog therapy. *Baill. Clin. Endocrin. Metabol.* **1999**, *13*, 409−18.

(6) (a) O'Byrne, K. J.; Carney, D. N. Radiolabeled somatostatin analogue scintigraphy in oncology. *Anticancer Drugs* **1996**, *7*, 33−44. (b) The trademark name for [^{111}In-DTPA^0]octreotide is Octreoscan.

(7) (a) Blum, J. E.; Handmaker, H.; Rinne, N. A. The utility of a somatostatin-type receptor binding peptide radiopharmaceutical (P829) in the evaluation of solitary pulmonary nodules. *Chest* **1999**, *115*, 224−32. (b) Blum, J.; Handmaker, H.; Lister-James, J.; Rinne, N.; and the NeoTect Solitary Pulmonary Nodule Study Group. A multicenter trial with a somatostatin analog ^{99m}Tc depreotide in the evaluation of solitary pulmonary nodules. *Chest* **2000**, *117*, 1232−38. (c) Grewal, R. K.; Dadparver, S.; Yu, J. Q.; Babaria C. J.; Cavanaugh, T.; Sherman, M.; Jacobstein, J. Efficacy of Tc-99m depreotide scintigraphy in the evaluation of solitary pulmonary nodules. *Cancer J.* **2002**, *8*, 400−4. (d) The trademark name for ^{99m}Tc depreotide is NeoTect; NeoSpect in Europe.

(8) Otte, A.; Jermann, E.; Behe, M.; Goetze, M.; Bucher, H. C.; Roser, H. W.; Heppeler, A.; Mueller-Brand, J.; Maecke, H. R. DOTATOC: a powerful new tool for receptor-mediated radionuclide therapy. *Eur. J. Nucl. Med.* **1997**, *24*, 792−5.

(9) Stolz, B.; Weckbecker, G.; Smith-Jones, P. M.; Albert, R.; Raulf, F.; Bruns, C. The somatostatin receptor-targeted radiotherapeutic [^{90}Y-DOTA-D-Phe^1, Tyr^3]octreotide (90Y-SMT 487) eradicates experimental rat pancreatic CA 20948 tumours. *Eur. J. Nucl. Med.* **1998**, *25*, 668−74.

(10) de Jong, M.; Breeman, W. A. P.; Bernard, B. F.; Bakker, W. H.; Schaar, M.; van Gameren, A.; Bugaj, J. E.; Erion, J.; Schmidt, M.; Srinivasan, A.; Krenning, E. P. [^{177}Lu-DOTA^0, Tyr^3]Octreotate for somatostatin receptor-targeted radionuclide therapy. *Int. J. Cancer* **2001**, *92*, 628−33.

(11) de Jong, M.; Breeman, W. A.; Bernard, B. F.; Rolleman, E. J.; Hofland, L. J.; Visser, T. J.; Setyono-Han, B.; Bakker, W. H.; van der Pluijm M. E.; Krenning, E. P. Evaluation in vitro and in rats of ^{161}Tb-DTPA-octreotide, a somatostatin analogue with potential for intraoperative scanning and radiotherapy. *Eur. J. Nucl. Med.* **1995**, *22*, 608−16.

(12) Lewis, J. S.; Lewis, M. R.; Srinivasan, A.; Schmidt, M. A.; Wang, J.; Anderson, C. J. Comparison of four ^{64}Cu-labeled somatostatin analogues in vitro and in a tumor-bearing rat model: evaluation of new derivatives for positron emission tomography imaging and targeted radiotherapy. *J. Med. Chem.* **1999**, *42*, 1341−7.

(13) Zamora, P. O.; Gulhke, S.; Bender, H.; Diekmann, D.; Rhodes, B. A.; Biersack, H. J.; Knapp, F. F., Jr. Experimental radiotherapy of receptor-positive human prostate adenocarcinoma with ^{188}Re-RC-160, a directly-radiolabeled somatostatin analogue. *Int. J. Cancer* **1996**, *65*, 214−20.

(14) (a) Wild, D.; Schmitt, J. S.; Ginj, M.; Maeke, H. R.; Bernard, B. F.; Krenning, E.; de Jong, M.; Wenger, S.; Reubi, J.-C. DOTA-NOC, a high affinity ligand of somatostatin receptor subtype 2, 3, and 5 for labelling with various radiometals. *Eur. J. Nucl. Med.* **2003**, *30*,

1338−47. (b) Ginj, M.; Chen, J.; Walter, M. A.; Eltschinger, V.; Reubi, J.-C.; Maeke, H. R. Preclinical evaluation of new and highly potent analogues of octreotide for predictive imaging and targeted radiotherapy. *Clin. Canc. Res.* **2005**, *11*, 1136−45.

(15) Bodei, L.; Cremonesi, M.; Zoboli, S.; Grana C.; Bartolomei, M.; Rocca, P.; Caracciolo, M.; Maecke, H. R.; Chinol, M.; Paganelli, G. Receptor-mediated radionuclide therapy with ^{90}Y-DOTATOC in association with amino acid infusion: a phase I study. *Eur. J. Nucl. Med.* **2003**, *30*, 207−16.

(16) Kwekkeboom, D. J.; Teunissen, J. J.; Bakker, W. H.; Kooij, P. P.; de Herder, W. W.; Feelders, R. A.; van Eijck, C. H.; Esser, J-P.; Kam, B. L.; Krenning, E. P. Radiolabeled somatostatin analog [^{177}Lu-DOTA^{0}, Tyr^{3}]octreotate in patients with endocrine gastroenteropancreatic tumors. *J. Clin. Oncol.* **2005**, *23*, 2754−62.

(17) (a) Pearson, D. A.; Lister-James, J.; McBride, W. J.; Wilson, D. M.; Martel, L. J.; Civitello, E. R.; Taylor, J. E.; Moyer, B. R.; Dean, R. T. Somatostatin receptor-binding peptides labeled with technetium-99m: chemistry and initial biological studies. *J. Med. Chem.* **1996**, *39*, 1361−71. (b) Cyr, J. E.; Pearson, D. A.; Nelson, C. A.; Lyons, B. A.; Zheng, Y.; Bartis, J.; He, J.; Cantorias, M. V.; Howell, R. C.; Francesconi, L. F. Isolation, characterization, and biological evaluation of syn and anti diastereomers of Tc 99m depreotide: a somatostatin receptor binding imaging agent. *J. Med. Chem.*, in press.

(18) Deutsch, E.; Libson, K.; Vanderheyden, J-L.; Ketring, A. R.; Maxon, H. R. The chemistry of rhenium and technetium as related to the use of isotopes of these elements in therapeutic and diagnostic nuclear medicine. *Int. J. Radiat. Appl. Inst. B Nucl. Med. Biol.* **1986**, *13*, 465−77.

(19) Guhlke, S.; Beets, A. L.; Oetjen, K.; Mirzadeh, S.; Biersack, H-J.;Knapp, F. F. Simple new method for effective concentration of ^{188}Re solutions from alumina-based ^{188}W-^{188}Re generator. *J. Nucl. Med.* **2000**, *41*, 1271−78.

(20) Review: Jeong, J. M.; Chung, J.-K. Therapy with 188Re-labeled radiopharmaceuticals: an overview of promising results from initial clinical trials. *Cancer Biother. Radiopharm.* **2003**, *18*, 707−17.

(21) Smith, C. J.; Sieckman, G. L.; Owen, N. K.; Hayes, D. L.; Mazuru, D. G.; Volkert, W. A.; Hoffman, T. J. Radiochemical investigations of [188Re(H2O)(CO)3-diaminopropionic acid-SSS-bombesin(7−14)-NH2]: Synthesis, radiolabeling and in vitro/in vivo GRP receptor targeting studies. *Anticancer Res.* **2003**, *23*, 63−70.

(22) Miao, Y.; Owen, N. K.; Fisher, D. R.; Hoffman, T. J.; Quinn, T. P. Therapeutic efficacy of a ^{188}Re-labeled a-melanocyte-stimulating hormone peptide analog in murine and human melanoma-bearing mouse models. *J. Nucl. Med.* **2004**, *46*, 121−9.

(23) Results not published but presented. Abstract: Azure, M. T.; Jones, W. B.; Cyr, J. E., De Rosch, M. A., Zinn, K. R., Bush, L. R. High specific activity rhenium-188 labeled somatostain analogs for tumor eradication. *Book of Abstracts*, 217th American Chemical Society National Meeting, Anaheim, CA, Mar 21−25, 1999; American Chemical Society: Washington, DC, 1999.

(24) Lambert, B.; Cybulla, M.; Weiner, S. M.; Van De Wiele, C.; Ham H.; Dierckx, R. A.; Otte, A. Renal toxicity after radionuclide therapy. *Radiat. Res*. **2004**, *161*, 607−11.

(25) Rolleman, E. J.; Valkema, R.; de Jong, M.; Kooij, P. P. M.; Krenning, E. P. Safe and effective inhibition of renal uptake of radiolabelled octreotide by combination of lysine and arginine. *Eur. J. Nucl. Med.* **2003**, *30*, 9−15.

(26) (a) Grummon, G.; Rajagopalan, R.; Palenik, G. J.; Koziol, A. E.; Nosco, D. L. Synthesis, Characterization and Crystal Structures of Technetium(V)-Oxo Complexes Useful in Nuclear Medicine. 1. Complexes of Mercaptoacetylglycylglycylglycine (MAG_3) and its methyl ester derivative (MAG_3OMe). *Inorg. Chem.* **1995**, *34*, 1764−72. (b) Wong, E.; Fauconnier, T.; Bennett, S.; Valliant, J.; Nguyen, T.; Lau, F.; Lu L. F. L.; Pollak, A.; Bell, R. A.; Thornback, J. R. Rhenium(V) and Technetium(V) Oxo Complexes of an $N_2N'S$ Peptidic Chelator: Evidence of Interconversion between the Syn and Anti Conformations. *Inorg. Chem.* **1997**, *36*, 5799−5808.

(27) Chan, W.; White, P. *Fmoc Solid Phase Peptide Synthesis: a Practical Approach*; Oxford University Press: Oxford, 2000.

(28) Barlos, K.; Gatos, D.; Kallitsis, J.; Papaphotiu, G.; Sotiriu, P.; Wenqing, Y.; Schaefer, W. Darstellung geschuetzter peptid-fragmente unter einsatz substituierter triphenylmethyl-harze. *Tetrahedron. Lett.* **1989**, *30*, 3943−6.

(29) Carpino, L. A. 1-Hydroxy-7-azabenzotriazole. An efficient peptide coupling additive. *J. Am. Chem. Soc.* **1993**, *115*, 4397−8.

(30) Rink, H. Solid-phase synthesis of protected peptide fragments using a trialkoxydiphenyl-methyl ester resin. *Tetrahedron Lett.* **1987**, *28*, 3787−90.

(31) (a) Pearson, D. A.; Blanchette, M.; Baker, M. L.; Guindon, C. A. Trialkylsilanes as scavengers for the trifluoroacetic acid deblocking of protecting groups in peptide synthesis. *Tetrahedron. Lett.* **1989**, *30*, 2739−42. (b) Bryson N.; Dewan J. C.; Lister-James, J.; Jones, A. G.; Davison, A. Neutral technetiun (V) complexes with amide-thiol-thioether chelating ligands. *Inorg. Chem.* **1988**; *27*, 2154−61.

(32) Froidevaux, S.; Hintermann, E.; Torok, M.; Macke, H. R.; Beglinger, C.; Eberle, A. N. Differential regulation of the somatostatin receptor Type 2 (sst2) expression in AR4−2J tumor cells implanted into mice during octreotide treatment. *Cancer Res.* **1999**, *59*, 3652−57.

(33) Taylor, J. E.; Theveniau, M. A.; Bashirzadeh, R.; Reisine, T.; Eden, P. A. Detection of somatostatin receptor subtype 2 (SSTR") in established tumors and tumor cell lines: evidence for SSTR2 heterogeneity. *Peptides* **1994**, *15*, 1229−36.

(34) Bylund, D. B.; Yamamura, H. I., *Methods for Receptor Binding in Methods in Neurotransmitter Receptor Analysis*; Yamamura, et al., Eds.; Raven Press; New York, 1990; pp 1−35.

(35) Lipowska, M.; Hansen L.; Xu, X.; Marzilli, P. A.; Taylor, A., Jr.; Marzilli, L. G. New N3S donor ligand small peptide analogues of the *N*-mercaptoacetyl-glycylglycylglycine ligand in the clinically used Tc-99m renal imaging agent: evidence for unusual amide oxygen coordination by two new ligands. *Inorg. Chem.* **2002**, *41*, 3032−41.

(36) Stephenson, K. A.; Banerjee, S. R.; Besanger, T.; Sogbein, O. O.; Levadala, M. K.; McFarlane, N.; Lemon, J. A.; Boreham, D. R.; Maresca, K. P.; Brennan, J. D.; Babich, J. W.; Zubieta, J.; Valliant, J. F. Bridging the gap between in vitro and in vivo imagining: Isostructural Re and ^{99m}Tc complexes for correlating fluorescence and radioimaging studies. *J. Am. Chem. Soc.* **2004**, *126*, 8598−9.

(37) Froidevaux, S.; Calame-Christe, M.; Tanner, H.; Eberle, A. N. Melanoma targeting with DOTA-alpha-melanocyte-stimulating hormaone analogs: structural parameters affecting tumor and kidney uptake. *J. Nucl. Med.* **2005**, *46*, 887−95.

(38) Wilbur, D. S.; Hamlin, D. K.; Sanderson, J.; Lin, Y. Streptavidin in antibody pretargeting. 4. Site-directed mutation provides evidence that both arginine and lysine residues are involved in kidney localization. *Bioconjugate Chem.* **2004**, *15*, 1454−63.

(39) Akizawa, H.; Arano, Y.; Mifune, M.; Iwado, A.; Saito, Y.; Mukai, T.; Uehara, T.; Ono, M.; Fujioka, Y.; Ogawa, K.; Kiso, Y.; Saji, H. Effect of molecular charges on renal uptake of ^{111}In-DTPA-conjuagated peptides. *Nucl. Med. Biol.* **2001**, *28*, 761−8.

(40) Han, Y.; Albericio, F.; Barany, G. Occurrence and minimization of cysteine racemization during stepwise solid-phase peptide synthesis. *J. Org. Chem.* **1997**, *62*, 4307−12.

JM061290I